

Scale Factor in Powder Diffraction

P. RIELLO,* G. FAGHERAZZI AND P. CANTON

Dipartimento di Chimica Fisica, Università di Venezia, DD2137, 30123 Venezia, Italy. E-mail: riellop@unive.it

(Received 3 March 1997; accepted 1 October 1997)

Abstract

In this paper, a simple method of obtaining the scale factor that transforms powder intensities from arbitrary units into electron units is proposed. This method, which is suitable for diffraction data collected from polycrystalline single-phase specimens, without fluorescence and preferred-orientation effects, obtains the scale factor analyzing the global scattered intensity in the reciprocal space without the necessity for the peak–background separation. Once the scale factor is found, it is possible to estimate the overall thermal parameter and to trace a physically based background line which is useful in extracting accurate structure factors.

1. Introduction

Several methods have been devised to convert the raw intensities on an absolute scale for single-crystal data. The classical method is based on the statistical analysis of reciprocal space and needs the knowledge of the chemical composition of the unit cell (Wilson, 1942). Other methods use the knowledge of a known structure whose molecule is similar to the given compound (Parthasarathy & Sekar, 1993) or the Fourier inverse of the Patterson origin (Blessing & Langs, 1988). Moreover, other sophisticated methods exist for large molecules and proteins (Roth, 1986; Subramanian & Hall, 1982).

Several methods (Chipman, 1969; Steven & Coppens, 1975) exist to scale the relative structure factors for crystalline powder diffraction data but they need the use of careful experimental procedures, not only for the measurement of the primary beam power P_0 but also for the measurement of the volume and the weight of the sample; for this reason, they are not very common. Usually, when investigating powder diffraction data, Wilson's method is applied because it requires quantities (*i.e.* global scattering intensities inside a spherical shell of the reciprocal space) that do not depend on the decomposition of the overlapping reflections. However, the peak–background separation sometimes biases the estimated parameters (especially the overall temperature factor B).

We are proposing a simple method that is suitable for powder diffraction data that have been collected from polycrystalline single-phase specimens, without fluorescence effects, in order to obtain the scale factor that

transforms the numerical values of the experimental intensities from arbitrary units into electron units. This normalization factor is useful in the estimation of the scale factor in the initial stage of the Rietveld refinement and in extracting accurate structure factors from powder data which are useful when applying direct methods. Our method needs prior knowledge of the unit-cell composition, like the Wilson one, and of the unit-cell volume. Unlike the Wilson plot, it gives the scale factor K separated (and therefore not strongly correlated) from the temperature factor B and does not need the peak–background separation.

2. Theory

The kinematic scattering amplitude for N atoms is

$$A(\mathbf{s}) = \iiint \sum_{i=1}^N \rho_i(\mathbf{x} - \mathbf{x}_i) \exp(i\mathbf{x} \cdot \mathbf{s}), \quad (1)$$

where $\rho_i(\mathbf{x} - \mathbf{x}_i)$ is the electron density of the i th atom at the position x_i .

Parseval's theorem states that the total intensity in the reciprocal space is given by

$$\begin{aligned} \iiint I(\mathbf{s}) \, d\mathbf{s} &= \iiint |A(\mathbf{s})|^2 \, d\mathbf{s} \\ &= \iiint \sum_{ij} \rho_i(\mathbf{x} - \mathbf{x}_i) \rho_j(\mathbf{x} - \mathbf{x}_j) \, d\mathbf{x} \end{aligned} \quad (2)$$

and if the electronic densities of the atoms are not overlapped (atomicity),

$$\rho_i(\mathbf{x} - \mathbf{x}_i) \rho_j(\mathbf{x} - \mathbf{x}_j) = \delta_{ij} \rho^2(\mathbf{x} - \mathbf{x}_j), \quad (3)$$

we obtain

$$\iiint I(\mathbf{s}) \, d\mathbf{s} = \sum_i^N \iiint \rho_i^2(\mathbf{x} - \mathbf{x}_i) \, d\mathbf{x} = \iiint \sum_i^N |f_i^o(\mathbf{s})|^2 \, d\mathbf{s}, \quad (4)$$

where $f_i^o(\mathbf{s})$ is the i th atomic scattering factor. The validity of (4) is only related to the atomicity hypothesis and does not depend on the spatial atomic arrangement.

Equation (4) is not useful for obtaining the scale factor in standard single-crystal analyses because it requires the knowledge of the diffraction intensities in all the reciprocal space, while the intensities are usually collected only on the reciprocal lattice.

Table 1. Symbols used in equations (5a) and (5b)

K	Global scale factor
A	Correction factor for absorption
P	Polarization factor (depending also on the monochromator set-up)
J_k	Multiplicity factor
L_k	Lorentz factor, $[\sin^2(\theta_k) \cos(\theta_k)]^{-1}$
$ F_k ^2$	Squared structure factor for the k th reflection, including the Debye-Waller factor
$\Phi(2\theta - 2\theta_k)$	Profile functions, including asymmetry correction, normalized if 2θ is expressed in degrees
V_c	Unit-cell volume
λ	Wavelength of the characteristic radiation used
B	Overall thermal factor
I^{coh}	Independent coherent scattering, given by $\sum_{\text{cell}} f_j^o ^2$. The sum is extended to all atoms contained in the unit cell
I^{inc}	Compton scattering given by $\sum_{\text{cell}} I_j^{\text{inc}}$; I_j^{inc} can be evaluated using the analytical expression and the relevant parameters published by Smith <i>et al.</i> (1975). The incoherent scattering must be corrected for the Breit-Dirac factor, for specific absorption effects and for the band-pass function of the monochromator, if this is used on the diffracted beam (Ruland, 1961, 1964)
Y^{air}	Air contribution to the background; it can be evaluated using the experimental air scattering which has been corrected for the presence of the specimen (Ottani <i>et al.</i> 1993)

In powder diffraction, if no preferred orientation is present, the scattered intensity at the angle 2θ is averaged on a spherical shell, with radius $|s| = 2 \sin(\theta)/\lambda$, and this is sufficient in evaluating the integral (4):

$$\iiint I(\mathbf{s}) \, d\mathbf{s} = \int I(s) 4\pi s^2 \, ds = \int \sum_i^N |f_i^o(s)|^2 4\pi s^2 \, ds, \quad (4a)$$

where $f_i^o(s)$ are the tabulated atomic scattering factors.

In a laboratory powder X-ray diffraction experiment, the intensity data are usually collected with a θ - 2θ diffractometer which operates in a step-scan mode (equal steps in 2θ), with a monochromator or a filter that selects two incident X-ray wavelengths, *e.g.* $K\alpha_1$ - $K\alpha_2$ doublet, with intensity ratio $K\alpha_1/K\alpha_2$ of 2.

Recently, in the context of Rietveld analysis, we have found an expression for the intensity diffracted by a powder sample (Riello *et al.*, 1995), where the whole diffraction pattern is evaluated on a physical basis, taking into account the Bragg and the diffuse scattering (TDS plus static disorder, Compton and air scattering).

The value of the intensity Y diffracted at the 2θ diffraction angle is determined by summing up the contributions from the n_B neighboring Bragg reflections, each centered at the $2\theta_k$ angle, to the background (Y^{bk}) and to air scattering (Y^{air}):

$$Y = KAP \left[\sum_k^{n_B} J_k L_k |F_k|^2 \Phi(2\theta - 2\theta_k) + Y^{\text{bk}} \right] + Y^{\text{air}}, \quad (5a)$$

where

$$Y^{\text{bk}} = [(16\pi^2 V_c)/(180\lambda^3)] \times (I^{\text{inc}} + \{1 - \exp[-2B \sin^2(\theta)/\lambda^2]\} I^{\text{coh}}). \quad (5b)$$

The symbols used are given in Table 1.

The intensity reported in (5a), (5b) for a very disordered structure (*i.e.* $B \rightarrow \infty$) reduces to

$$\lim_{B \rightarrow \infty} Y = KAP [(16\pi^2 V_c)/(180\lambda^3)] (I^{\text{inc}} + I^{\text{coh}}) + Y^{\text{air}}. \quad (6)$$

In fact, because of an extremely high B value, the Debye-Waller factor cancels the Bragg contribution to the scattering intensity.

Our aim is to evaluate K , *i.e.* the scale factor necessary to convert the absolute intensities to the relative ones of the given powder experiment. An expression for K can be obtained by integrating Y , which has been corrected for air scattering, absorption and polarization, on the reciprocal space, taking into account that the integral does not depend on atomic ordering (*i.e.* B value):

$$(16\pi^2 V_c)/(180\lambda^3) K = \frac{\lim_{B \rightarrow \infty} \int_0^\infty [(Y - Y^{\text{air}})/AP] 4\pi s^2 \, ds}{\int_0^\infty (I^{\text{coh}} + I^{\text{inc}}) 4\pi s^2 \, ds} = \frac{\int_0^\infty [(Y - Y^{\text{air}})/AP] 4\pi s^2 \, ds}{\int_0^\infty (I^{\text{coh}} + I^{\text{inc}}) 4\pi s^2 \, ds}. \quad (7)$$

An alternative derivation, which uses the statistical properties of the intensities in the reciprocal space, is reported in Appendix A.

Equation (7), which bases itself only upon the atomicity hypothesis, is quite general although it was derived from (5a), (5b), which are valid for the uncorrelated disorder case. In fact, the integrals in the numerator of (7) do not depend on the atomic positions so they can be evaluated in the most convenient case.

A direct use of (7) is not possible because the experimental intensity Y^{exp} is not accessible in all the reciprocal space, so that the constant value of K can be obtained by following the same approach used by Vonk (1973) only as the limiting value for the ratio:

$$K(s_p) = [(180\lambda^3)/\frac{3}{2}(16\pi^2 V_c)] \lim_{s_p \rightarrow \infty} R(s_p), \quad (8)$$

where

$$R(s_p) \equiv \int_{s_{\text{min}}}^{s_p} Y^{\text{exp}} 4\pi s^2 \, ds / \int_{s_{\text{min}}}^{s_p} (I^{\text{coh}} + I^{\text{inc}}) 4\pi s^2 \, ds,$$

where Y^{exp} is the observed intensity that has been corrected for air scattering, absorption and polarization.

The factor $3/2$ has been introduced to take into account the presence of two radiation wavelengths with an intensity ratio of $1/2$. Obviously, the limit reported in (8) is biased by the extension of the actual measured reciprocal space. The trend of $K(s_p)$ is oscillatory and its asymptotic value might not be precisely defined especially if the peaks are still strong (*i.e.* for materials with low B) in the high- s region.

3. Experimental

XRD patterns were recorded at 295 K with a step size of 0.02° on a 10 – 140° range. The diffraction data were collected (10 s step^{-1}) using a Philips X'Pert system (PW3020 vertical goniometer and PW3710 MPD control unit) equipped with a focusing graphite monochromator on the diffracted beam and with a proportional counter (PW1711/90) with electronic pulse-height discrimination. We used a divergence slit of 0.5° , a receiving slit of 0.2 mm, and an anti-scatter slit of 0.5° Ni-filtered $\text{Cu K}\alpha$ radiation (30 mA, 40 kV).

This procedure for evaluating the global scale has been tested on four single-phase polycrystalline samples: α - Al_2O_3 , Y_2O_3 , α -quartz and Al.

The air scattering was collected (10 s step^{-1} and step size 0.5°) on the same 2θ range, fitted with a suitable

function (two pseudo-Voigt functions and a straight line) and subtracted from the raw data.

The monochromator on the diffracted beam also imposes a correction on incoherent scattering evaluated in the denominator of (7). Such a correction is obtained by using a band-pass function, characteristic of the instrument, which is necessary when considering the attenuation of the Compton intensity due to the monochromator. A fair determination of this function can be obtained by using a modified Rietveld refinement of some standard materials (Riello *et al.*, 1997).

The scale factors obtained by this procedure were compared with those refined by Rietveld analysis using the *DBWS-9600* computer program written by Sakthivel & Young (1990).

4. Results and discussion

The functions $[180\lambda^3/(16\pi^2V_c3/2)]R(s_p)$ and their average values in the region $s > 1 \text{ \AA}^{-1}$ are shown in Figs. 1 and 2 (also reported in Table 2) for the tested materials.

In order to obtain a good evaluation of the scale factor with this method, it is important to collect the diffraction data in an s range as large as possible and, generally, a better evaluation of the scale will be obtained by using materials that have high thermal parameters and in the presence of a lot of peaks (*i.e.* large unit cell). Since the

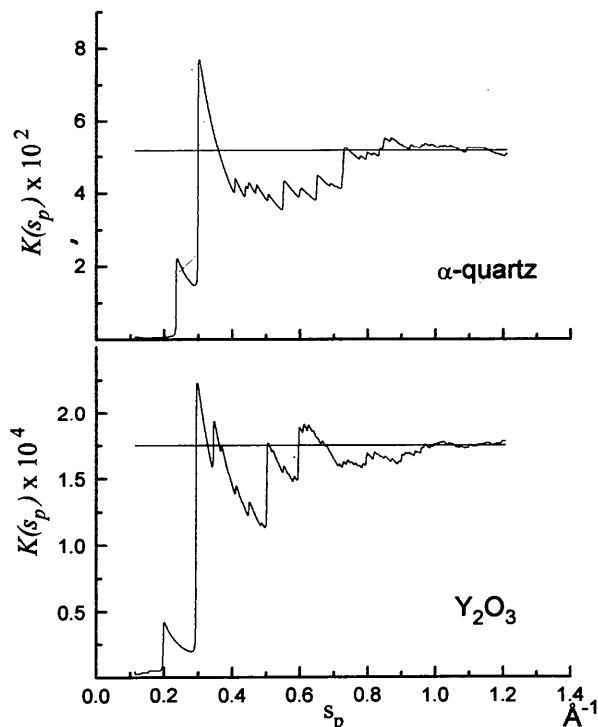


Fig. 1. Plot of the functions $K(s_p)$ vs s_p . The straight lines represent the mean values of $K(s_p)$ calculated for $s_p > 1 \text{ \AA}^{-1}$. Materials investigated: α -quartz and Y_2O_3 .

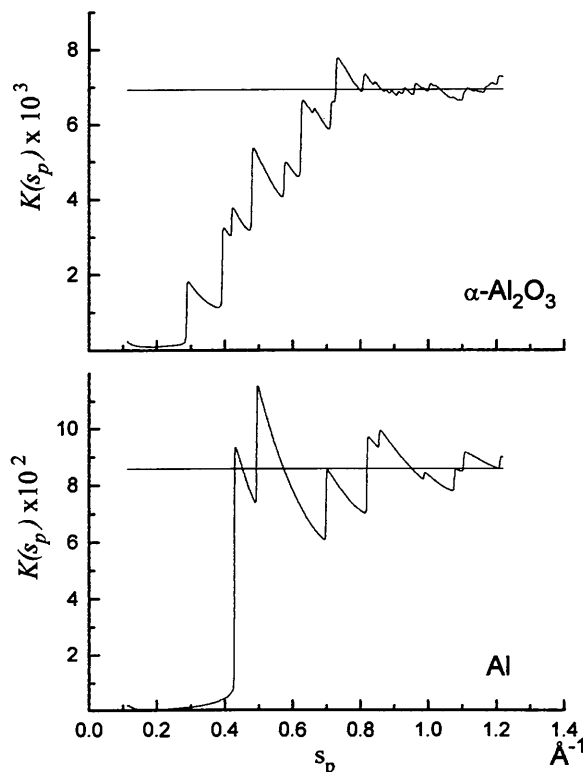


Fig. 2. As Fig. 1 but for α - Al_2O_3 and Al.

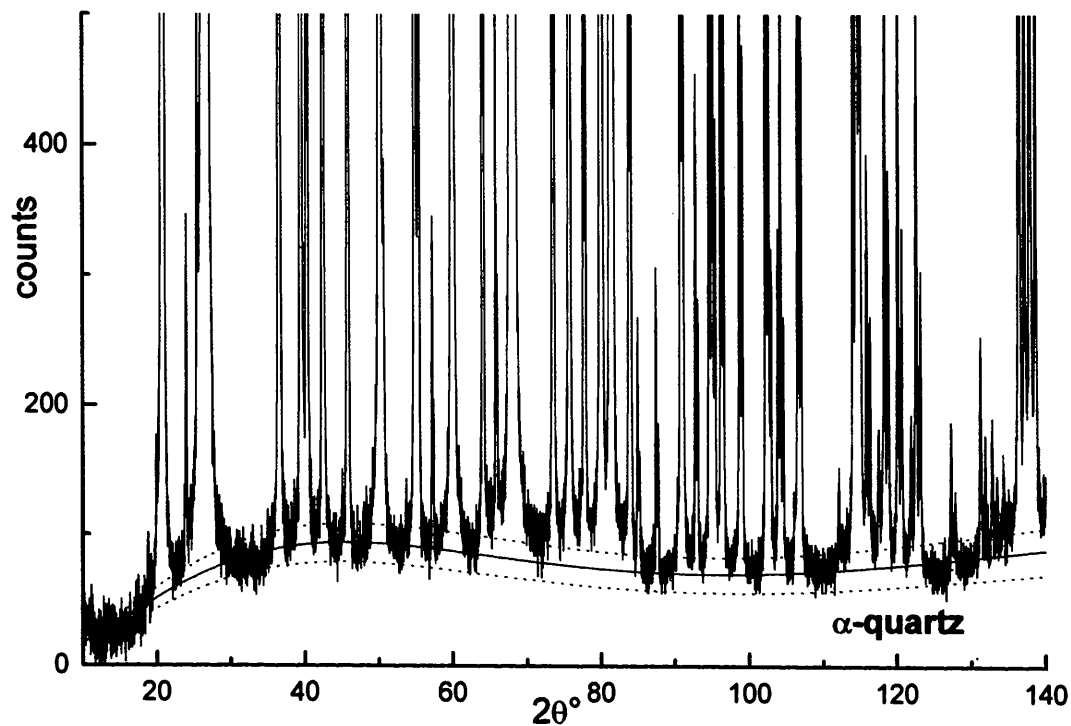


Fig. 3. Magnified XRD pattern of α -quartz. The diffraction pattern has been corrected for air scattering. The background solid line is obtained by formula (5b) with $B = 0.60 \text{ \AA}^2$ and $K = 5.17 \times 10^{-2}$. The dotted lines are the background evaluated respectively with $B = 0.4$ and $B = 0.8 \text{ \AA}^2$. The B value obtained by Rietveld analysis is 0.71 \AA^2 .

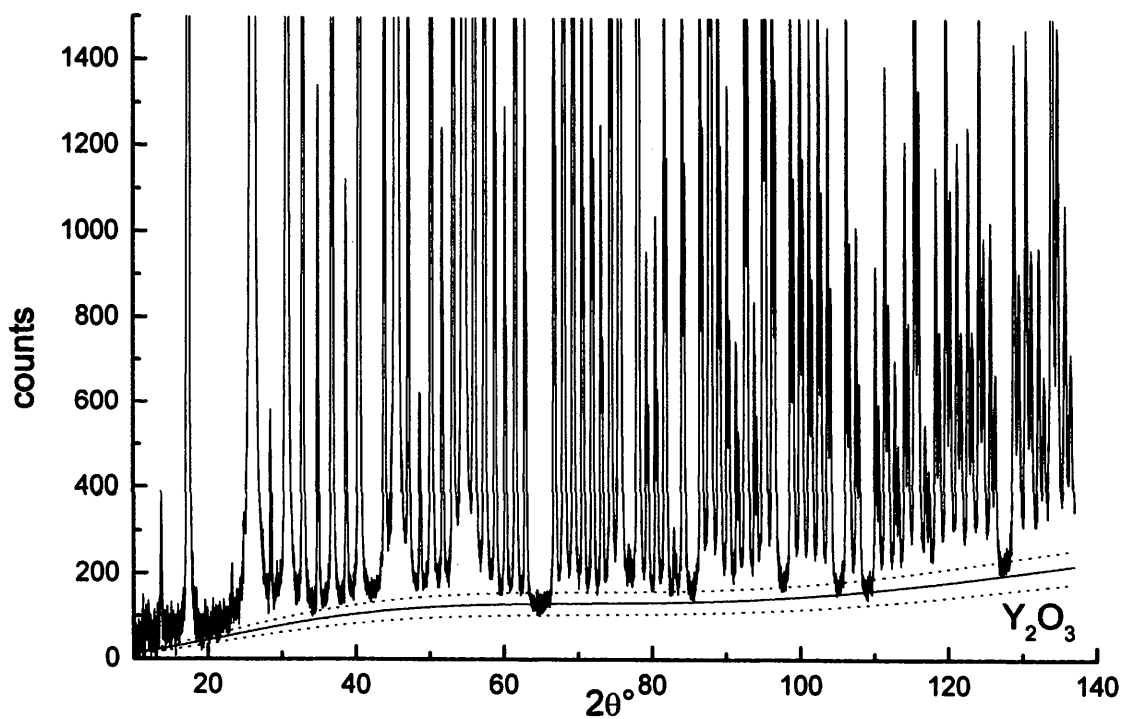


Fig. 4. As Fig. 3 but for Y_2O_3 . The solid line is obtained with $B = 0.5 \text{ \AA}^2$ and $K = 1.76 \times 10^{-4}$. The dotted lines are the background evaluated respectively with $B = 0.4$ and $B = 0.7 \text{ \AA}^2$. The B value obtained by Rietveld analysis is 0.55 \AA^2 .

Table 2. Comparison of the scale-factor values, K , obtained for different powder samples using the present method and the Rietveld refinement

The reported values correspond to the straight lines drawn in Figs. 1 and 2.

	α -Al ₂ O ₃	Al	α -Quartz	Y ₂ O ₃
Present method	6.94×10^{-3}	8.57×10^{-2}	5.17×10^{-2}	1.76×10^{-4}
Rietveld refinement	7.46×10^{-3}	8.37×10^{-2}	5.23×10^{-2}	1.84×10^{-4}

tested materials have low B values, they represent a severe test for this procedure.

In some cases, many oscillations are present in the high s_p region (Figs. 1 and 2) because of well defined and non-negligible crystalline peaks, but the obtained scale factors are close to those refined by using Rietveld analysis (Table 2), which shows the power of this method in determining the scale factor. The obtained values of the global scale factor are independent of the thermal parameter, whose value depends only on the separation between the peaks and the background.

Once the global scale factor K has been determined, it is possible to estimate B by searching for the value that gives a suitable background line $KAPY^{\text{bk}}$. In fact, this line, whose expression is reported in (5b), depends only on the thermal parameter when K has been found. Therefore, by a trial-and-error procedure, it is possible to select the B value that gives the best background line (Figs. 3 and 4).

5. Conclusions

The proposed integral method for the determination of the scale factor requires the prior knowledge of the unit-cell volume and chemical composition without any peak-background separation unlike the Wilson plot. In our procedure, the raw data must be corrected for absorption, polarization and air scattering and if the monochromator works on the diffracted beam it is necessary to know the band-pass function. Although, theoretically, this method gives optimal results for high- B materials, it furnishes a good estimate of the global scale also in less restrictive conditions as we have proved by means of the reported tests.

With respect to the Wilson plot, the present method determines the scale factor separately from the overall thermal parameter and permits a different procedure for the extraction of structure factors. Firstly, the scale factor is found, then the best background line, depending only on the thermal factor B , is chosen and, lastly, it is possible to evaluate the peak areas.

It is important to remember that the scale factor found by this procedure is correct if the peak areas are evaluated using the abscissa which has been measured in degrees.

Readers interested in the software should contact the first author.

APPENDIX A

An alternative way of obtaining (7) follows the same approach as used by Wilson (1942): we integrate the intensity (5a), (5b), which has been corrected for absorption, polarization and air scattering, in a shell of the reciprocal space.

The integration of the first part of (5a), *i.e.* the one relative to Bragg reflections, gives

$$\begin{aligned}
 & \int_{s_1}^{s_2} K \sum_k^{n_B} J_k L_k F_k^2 \Phi(2\theta - 2\theta_k) 4\pi s^2 ds \\
 &= \int_{\theta_1}^{\theta_2} K \sum_k^{n_B} J_k L_k F_k^2 \Phi(2\theta - 2\theta_k) (2/\lambda)^3 \\
 & \quad \times 4\pi \sin^2(\theta) \cos(\theta) d\theta \\
 &= K \sum' J_k F_k^2 \int_{\theta_1}^{\theta_2} [\sin^2(\theta_k) \cos(\theta_k)]^{-1} \Phi(2\theta - 2\theta_k) \\
 & \quad \times (2/\lambda)^3 4\pi \sin^2(\theta) \cos(\theta) d\theta. \quad (9)
 \end{aligned}$$

The symbol \sum' means that the sum is evaluated on all the reflections inside the integration shell.

Since $\sin^2(\theta) \cos(\theta)$ is gradually variable with respect to the profile peak functions, which are different from zero inside a very limited range, we can substitute it with the value assumed on the peak center $2\theta_k$ obtaining

$$\begin{aligned}
 & \sum' J_k F_k^2 \int_{\theta_1}^{\theta_2} \Phi(2\theta - 2\theta_k) (2/\lambda)^3 4\pi d\theta \\
 &= \sum' J_k F_k^2 \int_{\theta_1^{\theta_k}}^{\theta_2^{\theta_k}} \Phi(2\theta^{\circ} - 2\theta_k^{\circ}) (2/\lambda)^3 4\pi (\pi/360) d(2\theta^{\circ}), \quad (10)
 \end{aligned}$$

where we have taken into account that (5a), (5b) (and the constants there reported) are written for a profile peak function Φ normalized in the variable $2\theta^{\circ}$, measured in degrees, while the integral in (9) is expressed in radians, so obtaining

$$\begin{aligned}
 & \int_{s_1}^{s_2} \sum_k^{n_B} J_k L_k F_k^2 \Phi(2\theta - 2\theta_k) 4\pi s^2 ds \\
 &= (2/\lambda)^3 4\pi (\pi/360) \sum' J_k F_k^2. \quad (11)
 \end{aligned}$$

The average intensity of a general reflection, when evaluated on all the reciprocal lattice and not only for the reflections that actually appear, is independent of the symmetry (Wilson, 1949, 1950) and its value is given by

$$\sum' J_k F_k^2 / N = \sum_f^{\text{cell}} (|f_j^{\circ}|^2 \exp[-2B \sin^2(\theta)/\lambda^2]), \quad (12)$$

where $\langle \rangle$ denotes a mean value, $N = (4/3)\pi(s_2^3 - s_1^3)/V_r$ is the number of lattice points inside the considered shell and $V_r = 1/V_c$ is the volume of the reciprocal unit cell.

The integral of the Bragg contribution to (5a) on the considered shell is

$$\begin{aligned} I1 &\equiv \int_{s_1}^{s_2} K \sum_k^{n_B} J_k L_k F_k^2 \Phi(2\theta - 2\theta_k) 4\pi s^2 ds \\ &= K(2/\lambda)^3 (4\pi^2/360) (4/3)\pi(s_2^3 - s_1^3) V_c \\ &\quad \times \sum_j^{\text{cell}} (|f_j^o|^2 \exp[-2B \sin^2(\theta)/\lambda^2]). \quad (13) \end{aligned}$$

The integral of the second part of (5a), i.e. the one relative to disorder plus TDS [see (5b)], gives

$$\begin{aligned} I2 &\equiv \int_{s_1}^{s_2} K[(16\pi^2 V_c)/(180\lambda^3)] \{1 - \exp[-2B \sin^2(\theta)/\lambda^2]\} \\ &\quad \times \sum_j^{\text{cell}} |f_j^o|^2 4\pi s^2 ds \\ &= K[(16\pi^2 V_c)/(180\lambda^3)] (4/3)\pi(s_2^3 - s_1^3) \\ &\quad \times \left\{1 - \exp[-2B \sin^2(\theta)/\lambda^2]\right\} \sum_j^{\text{cell}} |f_j^o|^2. \quad (14) \end{aligned}$$

So for every shell the integral of Bragg and disorder plus TDS scattering does not depend on the B factor. In fact it gives

$$\begin{aligned} I1 + I2 &= K[(16\pi^2 V_c)/(180\lambda^3)] (4/3)\pi(s_2^3 - s_1^3) \left(\sum_j^{\text{cell}} |f_j^o|^2\right) \\ &= \int_{s_1}^{s_2} K[(16\pi^2 V_c)/(180\lambda^3)] \sum_j^{\text{cell}} |f_j^o|^2 4\pi s^2 ds \quad (15) \end{aligned}$$

and we can conclude that

$$\begin{aligned} &\int_0^\infty [(Y - Y^{\text{air}})/AP] 4\pi s^2 ds \\ &= K[(16\pi^2 V_c)/(180\lambda^3)] \\ &\quad \times \int_0^\infty \left(\sum_j^{\text{cell}} |f_j^o|^2 + \sum_j^{\text{cell}} I_j^{\text{inc}}\right) 4\pi s^2 ds. \quad (16) \end{aligned}$$

We thank Professor D. Clemente for useful discussions and suggestions. We thank CNR and MURST for financial support.

References

- Blessing, R. H. & Langs, D. A. (1988). *Acta Cryst.* **A44**, 729–735.
 Chipman, D. (1969). *Acta Cryst.* **A25**, 209–213.
 Ottani, S., Riello, P. & Polizzi, S. (1993). *Powder Diffr.* **8**, 149–154.
 Parthasarathy, S. & Sekar, K. (1993). *Acta Cryst.* **A49**, 389–398.
 Riello, P., Canton, P. & Fagherazzi, G. (1997). *Powder Diffr.* **12**, 160–166.
 Riello, P., Fagherazzi, G., Clemente, D. & Canton, P. (1995). *J. Appl. Cryst.* **28**, 115–120.
 Roth, M. (1986). *Acta Cryst.* **A42**, 230–240.
 Ruland, W. (1961). *Acta Cryst.* **14**, 1180–1185.
 Ruland, W. (1964). *Br. J. Appl. Phys.* **15**, 1301–1307.
 Sakthivel, A. & Young, R. (1990). *User's Guide to Programs DBWS-9600PC*. Georgia Institute of Technology, Atlanta, GA, USA.
 Smith, V. H. Jr, Thakkar, A. J. & Chapman, D. C. (1975). *Acta Cryst.* **A31**, 391–392.
 Steven, E. D. & Coppens, P. (1975). *Acta Cryst.* **A31**, 612–619.
 Subramanian, V. & Hall, R. (1982). *Acta Cryst.* **A38**, 577–590, 590–598, 598–608.
 Vonk, C. G. (1973). *J. Appl. Cryst.* **6**, 148–152.
 Wilson, A. J. C. (1942). *Nature (London)*, **150**, 152–154.
 Wilson, A. J. C. (1949). *Acta Cryst.* **2**, 318–321.
 Wilson, A. J. C. (1950). *Acta Cryst.* **3**, 258–261.